FOSSEE, IIT Bombay
OpenFOAM Case Study Project
April 20, 2021

Flow over a cylinder with rotating control cylinders in tandem

Maitreya Sinha
Indian Institute of Technology, Bombay

Abstract

In this study, we present the analysis of flow around a rigid cylinder with two small rotating cylinders located at a small distance. The vortices generated by the separation of the flow around the bluff cylindrical body are damped out by the momentum that is being injected by the two rotating cylinders. This causes the maximum lift and drag to be reduced, and makes the wake of the flow smaller. This type of flow control to delay separation of flow is called moving surface boundary layer control (MSBC). Computational analysis at Reynolds number ranging from 100 to 500 are used to simulate the flow for various rotational speeds of the control cylinders. The parameters of interest such as the Lift and Drag are used to validate the results. We study both the flow around a static and an oscillating cylinder in a uniform flow.

1 Introduction

In 1904 Prandtl had described the existence of boundary layer, and had begun the study of flow separation from bluff bodies. It has since been subject of investigation by researchers throughout the 20th century. [5]. In 1925, Prandtl had shown separation control via the rotation of circular cylinders.

Flow separation control techniques generally fall in one of two categories. When the delay in separation is being done purely by modifying the shape and surface characteristics, it is called passive flow separation techniques. Alternatively, when external power and actuation is being provided, called active flow separation techniques. In the present study, the control cylinders insert momentum into the flow near the boundary layer, and cause the flow to get reattached to the surface which allows for higher pressure recovery and lower pressure drag. Experiments done by Korkischko and Meneghini have shown that the vortex induced vibrations that are generated by the flow are also suppressed by the rotation of control cylinders in the proximity of a larger cylinder [2]. The suppression of large hydrodynamic forces that are generated on bluff bodies due to flows ranging from moderate to high reynolds numbers is advantageous to industrial applications where structural integrity is threatened due to flow

instabilities. Automotive and Aerospace industries also deal with vortex induced vibrations that cause design difficulties, and benefit greatly from control strategies that reduce drag and instabilities[4].

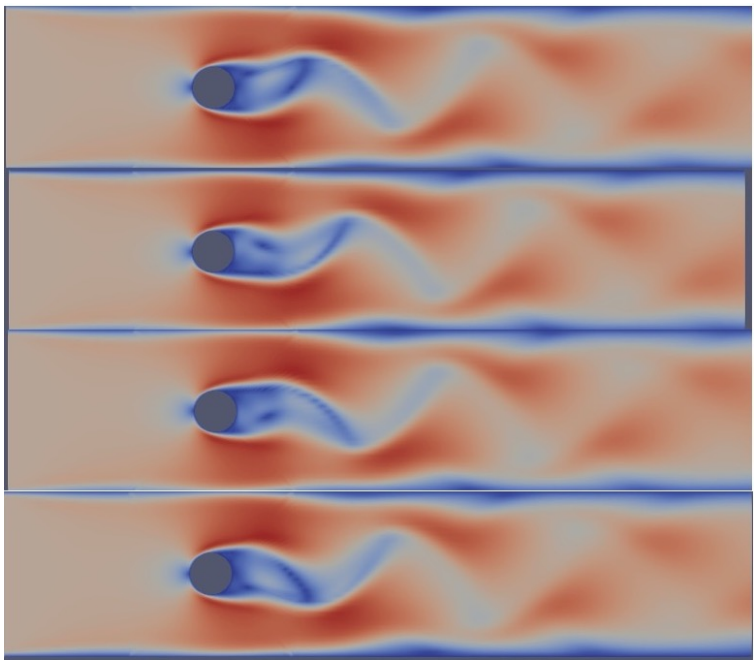

Figure 1: Vortices formed in flow over a cylinder

The current problem statement will be discussed in detail in section 2. We discuss the governing equations and theoretical models in section 3. The detailed description and dimensions of the domain and the flow geometry are discussed in section 4.1. The boundary conditions and the initial conditions that have been considered are discussed in section 4.2. Finally the solver used is mentioned in section 4.3. Finally the results of the analysis are discussed in section 5.

2 Problem Statement

Consider a domain, where a fluid is flowing over a cylinder as shown in Figure 2. As the steady state is reached, vortices are generated from the flow that is separating from the cylinder as shown in figure 1. The formation of vortices gives rise to an unsteady force whose components are the lift force, acting perpendicular to the flow. And the drag force acting in the direction of the flow. As the vortices are generated from the upper and the lower surface of the cylinder, the lift and the drag force is oscillates about their mean value[1]. In the absence of any other external force, the mean lift force is 0. For a specific value of reynolds number, we can obtain the lift coefficient C_l by the formula $C_l = \frac{F_{lift}}{\frac{1}{2}\rho U^2}$. Similarly the drag coefficient C_d can be obtained by $C_d = \frac{F_{drag}}{\frac{1}{2}\rho U^2}$. Here, F_{lift} and F_{drag} are the lift and drag

respectively. ρ is the density of the freestream fluid, and U_∞ is the velocity of the freestream.

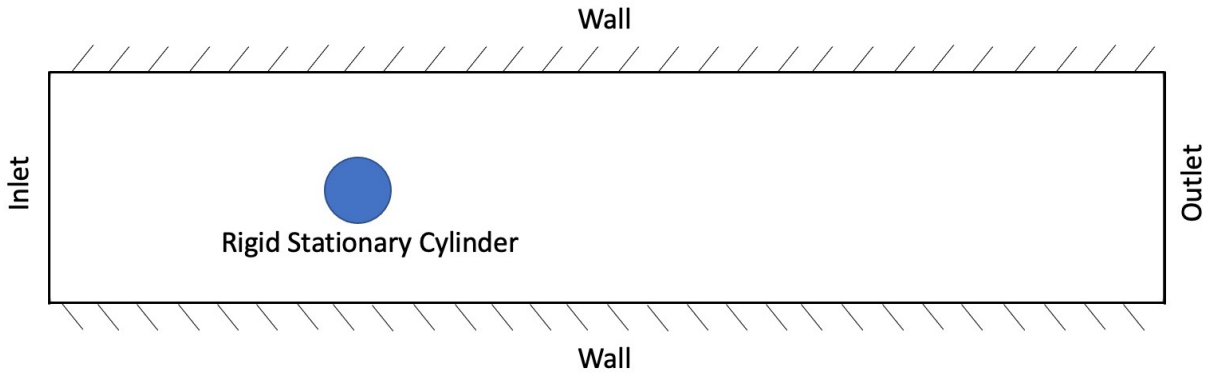

Figure 2: Representative domain of flow over a cylinder

The rotation velocity can be non-dimensionalized by the relationship $\xi = \frac{U_r}{U}$ Here ξ refers to the non dimensional velocity of rotation. U_r refers to the tangential velocity of the control cylinders and U refers to the free stream velocity. We study the problem for ξ in the range from 0 to 5.

3 Governing Equations

The main governing equation is the Navier-Stokes equation. We assume the flow to be viscous and incompressible.

$$\frac{\partial \mathbf{u}}{\partial t} + (\mathbf{u} \cdot \nabla)\mathbf{u} = -\frac{1}{\rho}\nabla p + \gamma \nabla^2 \mathbf{u} \tag{1}$$

Normalising the navier stokes equations using cylinder diameter (D_{cyl}) as the length scale, inlet velocity as the velocity scale U_∞, and $\tau = \frac{D_{cyl}}{U_\infty}$ as the time scale, we get

$$\frac{\partial u}{\partial \tau} + u\frac{\partial u}{\partial x} + v\frac{\partial u}{\partial y} = -\frac{\partial p}{\partial x} + \frac{1}{Re}(\frac{\partial^2 u}{\partial x^2} + \frac{\partial^2 u}{\partial y^2}) \tag{2}$$

$$\frac{\partial v}{\partial \tau} + u\frac{\partial v}{\partial x} + v\frac{\partial v}{\partial y} = -\frac{\partial p}{\partial y} + \frac{1}{Re}(\frac{\partial^2 v}{\partial x^2} + \frac{\partial^2 v}{\partial y^2}) \tag{3}$$

From mass conservation, we can also write

$$\frac{\partial u}{\partial x} + \frac{\partial v}{\partial y} = 0 \tag{4}$$

To quantify the forces, we formulate the stress tensor as the sum of its isotropic and deviatoric parts [3]:

$$\sigma = -\rho\mathbf{I} + \mathbf{T}, \quad \mathbf{T} = 2\mu\varepsilon(\mathbf{u}), \quad \varepsilon(\mathbf{u}) = \frac{1}{2}((\nabla\mathbf{u}) + (\nabla\mathbf{u})^T), \tag{5}$$

To obtain the force on the cylinder, we integrate the stress acting on an infinitesimal patch of area, and take the component of that force in the direction required[3].

$$C_d = \frac{1}{\frac{1}{2}\rho U^2 D} \int_{\Gamma_{cyl}} (\sigma n\cdot) \cdot n_x d\Gamma \tag{6}$$

$$C_l = \frac{1}{\frac{1}{2}\rho U^2 D} \int_{\Gamma_{cyl}} (\sigma n\cdot) \cdot n_y d\Gamma \tag{7}$$

The other parameters of interest are

$$\text{Reynolds Number}, Re = \frac{U_\infty D}{\nu} \tag{8}$$

$$\text{Strouhal Number}, St = \frac{fD}{U_\infty} \tag{9}$$

4 Simulation Procedure

4.1 Geometry and Mesh

For executing the problem, we first designed a geometry and meshed it in GMSH. The domain of study with the appropriate patch names are shown in figure 5. To enable the parametric control without disturbing the variables governing the generation of the structured mesh, the mesh is divided into a structured and an unstructured mesh regions. The main block of the geometry has unstructured mesh at the vicinity of the cylinder and the control cylinders. Everywhere else, the geometry is structured with appropriate grading. This allows us to run simulations for different cases without having to rework the geometry manually.

The geometry is designed in a way to allow parametric control on the following.

- Angular position of the cylinders
- Mesh refinement at the vicinity of the main and control cylinders
- Diameter of the main cylinder
- Diameter of the control cylinder
- Dimension of the inner unstructured region
- Dimension of the block dimension
- Gap between the control cylinders and main cylinders

The oscillating mesh domain is designed with a static mesh region and a oscillating region as shown in Figure 6. The inlet boundary conditions are designed in the static region and the flow passes through the contact region to interact with the cylinder. The mesh implements the moving boundary conditions using

- **Toposet** : To allow openfoam to identify the moving mesh patches and the oscillating cellzone. It allows the solver to capture the flux through the contact patch, and identify the mesh regions that should be operated upon by the Arbitrary Mesh Interface (AMI) solver.
- **Create Baffles** : Thus utility allows the contact meshed region to be treated as a plane that allows the flow through it. This enables the solver to treat the contact patch in the static region to be divided into two regions, one flow region, and a blocked region. The flow region is directly in contact with the neighbouring contact patch, and the rest of the patch is termed as the blocked region. This allows the contact region to pass the fluid flow through to the oscillating region

The oscillating meshed domain is shown in Figure 4.

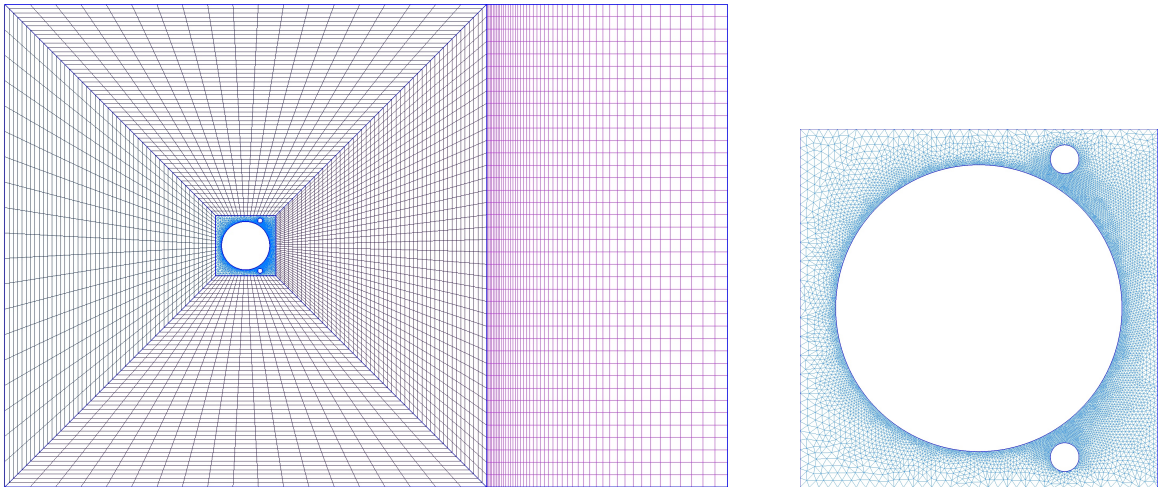

Figure 3: Overall mesh of the domain

The default values of the geometry and the mesh parameters are given in Table 1:

The parameters can be changed in the included .geo file in the Mesh folder of the case directory. The geometry is designed to be 2D, and a single cell is provided in the Z direction as per the solver requirements of OpenFOAM. The meshed geometry is exported in the msh22 format with 3D cells. A representative mesh generated with the cylinders in GMSH with the default mesh refinement factors produces 17798 nodes and 34608 elements. The overall mesh is shown in figure 3. A magnified view of the cylindrical region with the control cylinders is shown in figure 3 There is a second block downstream of the main block to capture the vortices. It has structured and graded mesh.

4.2 Initial and Boundary Conditions

The free stream velocity U_∞ is taken to be 10 m/s. At this velocity, they reynold's number (Re) = 1000. We can scale up the velocity to get the necessary reynolds number as required. The flow properties are given in Table 2.

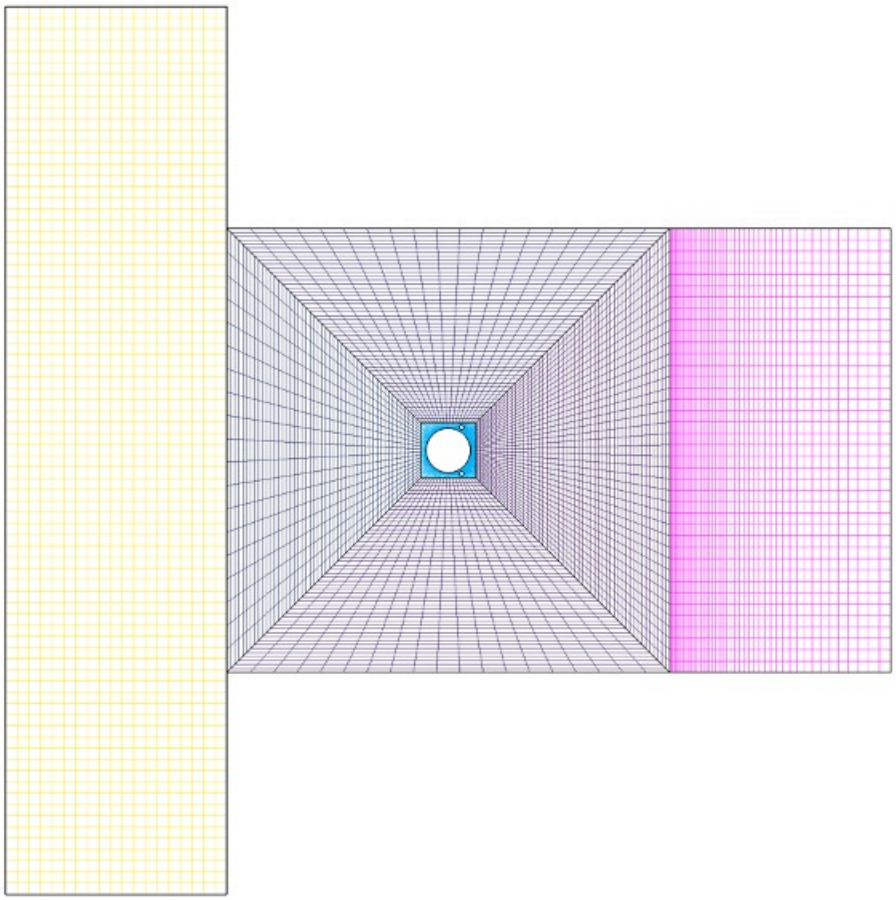

Figure 4: Mesh of the oscillating domain

$$\text{Reynolds Number, } Re = \frac{U_\infty D}{\nu} = \frac{10(m/s) * 1(m)}{10^{-2}(m^2/s)} = 1000.$$

The boundary conditions for each of the patches are given in Table 3.

The boundary conditions are set up in a way that there are no sudden change in velocities, and that the same graph can be used to study the flow conditions with and without control. At $t = 0$, the freestream velocity starts increasing till time t_0. After t_0, the freestream velocity remains constant. At this time, the control cylinders are stationary, and the flow stabilises for the conditions of no control. At a designated start time t_ω, the cylinders start rotating and the tangential velocity keeps increasing linearly from 0 to U_{tang} for a t_r or ramptime. After $t_\omega + t_r$, the cylinders keep rotating with a constant tangential velocity U_{tang}. This prevents any sudden velocity jumps and allows the solver to run with a finite Δt, and have a sensible courant number. For the default case, the value of t_0 is 1 sec, t_ω is 8 sec and t_r is 5 sec, U_{tang} is 30, and U_∞ is 10 m/s. This gives us the value $\xi = \frac{U_{tang}}{U_\infty}$ to be 3.

Geometry Dimension

Parameter	**Value**
Diamater of the main cylinder (D)	1 m
Diamater of the control cylinders (d)	0.1 m
Angle of the control cylinders with respect to the flow (θ)	60°
Length of the square domain / main block (L)	10 m
Length of the secondary block (L_ext)	5 m
Length of the secondary block (L_ext)	5 m

Mesh Parameters

Parameter	**Value**
Number of meshing points on the main block (y direction) before cylinder	20
Number of meshing points on the main block (y direction) after cylinder	50
Number of meshing points on the main block (x direction)	20
Number of meshing points on the secondary block (x direction)	50
Number of meshing points on the secondary block (y direction)	20
Main cylinder mesh refinement factor	0.01
Control cylinder mesh refinement factor	0.001

Table 1: Dimensions and mesh factors of the default geometry

Parameter	**Value**
Free stream velocity U_∞	10 m/s
Tangential rotational velocity U_{tang}	30 m/s
Density of fluid ρ	1.224 Kg/m^3
Kinematic viscocity ()	0.1 m$^2/s$
Transport model	Laminar

Table 2: Default flow properties

Boundary Conditions

Patch	**Boundary Conditions**	**Comments**
Inlet	$\mathrm{U}_\infty = \begin{cases} U_0 * t & \text{if } t < t_0, \\ U_0 & \text{otherwise.} \end{cases}$	Free stream velocity ramps up from 0 to U_0 in time t_0. The value of U_0 can be varied to obtain different values of reynolds numbers.
Outlet	Zero Gradient	
topAndBottom	slip	
frontAndBack	empty	patches in the z direction
mainCylinder	noSlip	
topControlCylinder	$\omega = \begin{cases} -U_{tang} * \frac{(t-t_\omega)}{t_r} & \text{if } t_\omega < t < (t_\omega + t_r), \\ -U_{tang} & \text{if } t > (t_\omega + t_r), \\ 0 & \text{otherwise.} \end{cases}$	$U_{tang} = \xi * U_\infty$ Thus U_{tang} can be varied to obtain different values of ξ
bottomControlCylinder	$\omega = \begin{cases} U_{tang} * \frac{(t-t_\omega)}{t_r} & \text{if } t_\omega < t < (t_\omega + t_r), \\ U_{tang} & \text{if } t > (t_\omega + t_r), \\ 0 & \text{otherwise.} \end{cases}$	

Table 3: Boundary Conditions

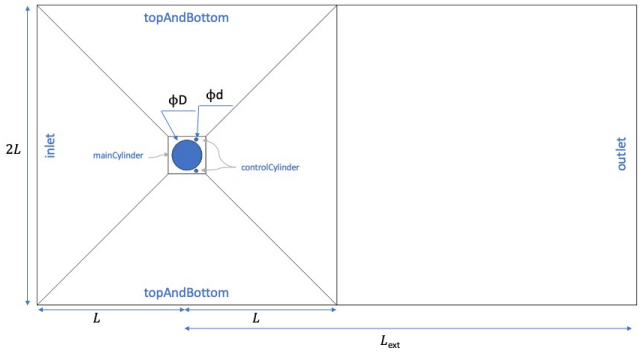

Figure 5: Geometry and patches of the domain being studied

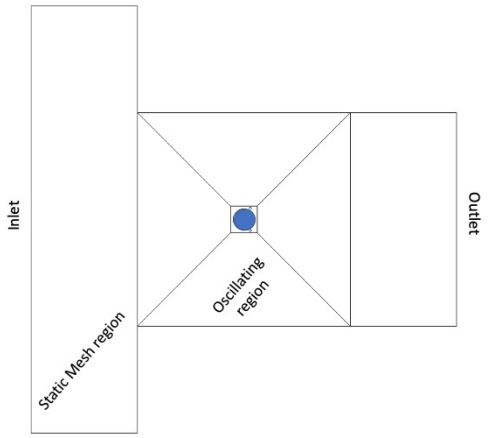

Figure 6: Geometry and patches of the oscillating domain being studied

4.3 Solver

We have used the **PimpleFoam** solver inside OpenFOAM to solve the equations. Pimplefoam is a transient solver that is designed for incompressible and turbulent / laminar flow of Newtonian fluids in a moving mesh. SIMPLE stands for Semi-Implicit Method for Pressure Linked Equations. In The SIMPLE algorithm, the velocity fields are iteratively solved using the pressure correction methods. In each iteration, there is a predictor step and a corrector step. Thus it iteratively obtains the velocity fields and keeps iterating till the velocity fields obtained changes by a value less than a given tolerance. PISO stands for Pressure Implicit with Splitting of Operator. PISO uses more corrector steps as compared to SIMPLE which gives it a more accurate solution as compared to SIMPLE. Thus it can even be used to study unsteady flows, and work with larger time steps. From the equation 4 we have

$$\nabla \cdot V = 0$$

From the momentum conservation equations, we have

$$\frac{\partial U}{\partial t} + U \cdot \nabla U - \nabla \cdot \nu \nabla U = -\nabla p$$

We discretise the momentum equation and obtain the algebraic equations of the form

$$M[u] = -\nabla p$$

where the matrix M[**u**] contains the diagonal and the off diagonal contributions via the formulation

$$M[u] = A\mathbf{u} - \mathbf{H}$$

Thus we finally obtain the discretised momentum equation

$$A\mathbf{u} - \mathbf{H} = \nabla p$$

on rearranging, we obtain the **velocity correction equation**

$$\mathbf{u} = \frac{\mathbf{H}}{A} - \frac{1}{A}\nabla p.$$

5 Results and Discussions

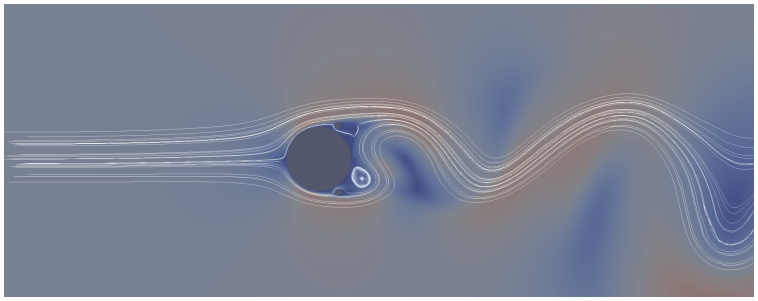

Figure 7: Streamlines of vortices being generated at $\xi = 0$

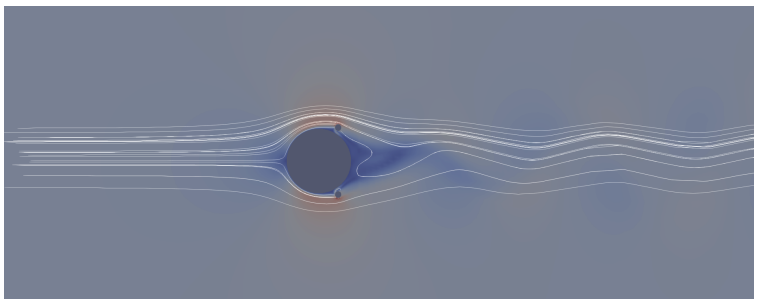

Figure 8: Streamlines of vortices being generated at $\xi = 3$

Case	$U_{tang}/U_\infty = 0$	$U_{tang}/U_\infty = 3$	$U_{tang}/U_\infty = 5$
$C_D(actual)$	1.51 ±0.15	0.77 ±0.11	0.49 ±0.10
Drag obtained (N)	722.2	461.56	240.12
$C_D(obtained)$	1.31	0.83	0.436

Table 4: Validation of mean drag coefficient with the paper [2]

5.1 Validation

We validate our simulations with the Numerical and Experimental Analysis of the same problem done by Korkischko and Meneghini [2]. We ran our simulation at Re = 3000, and have compared our mean drag coefficient with the results obtained by Korkischko and Meneghini at the same Re. The comparison is shown in the Table 4. The data is excellent acceptance of our results, and shows that the simulation is realistic. We increased our freestream velocity to 30m/s for the validation, keeping all other parameters to the default values.

Using the relation

$$C_d = \frac{F_{drag}}{\frac{1}{2}\rho U^2 D}$$

we can obtain the mean drag coefficients.

5.2 Grid Sensitivity

For the grid convergence study, we remesh the geometry with different paramteres such that we have 18982 nodes 33840 elements. The simulation was rerun for Re=1000 and $\xi = 2$. The comparison for the results obtained is plotted in Figure 9.

5.3 Parametric Results

We present the results we obtained for Re = 1000 and Re = 3000, and $\xi = 0$, $\xi = 3$ and $\xi = 5$ in Figures 10, 11 and 12

6 Conclusion

We observe that this method of control, where we rotate two small cylinders in proximity to a static cylinder can significantly reduce the lift amplitude as well as the mean drag. The cylinders inject momentum into the wake, and thus damp the fluctuating velocities and pressures. This reduces the recirculation region and suppresses the vortex induced vibrations that are formed.

We note that the rotating cylinders inject power into the boundary layers, that cause them to reattach to the static cylinder surface. The injected momentum flux causes the streamlines to reattach at a higher pressure, and thus reduce pressure drag. Due to the separation of

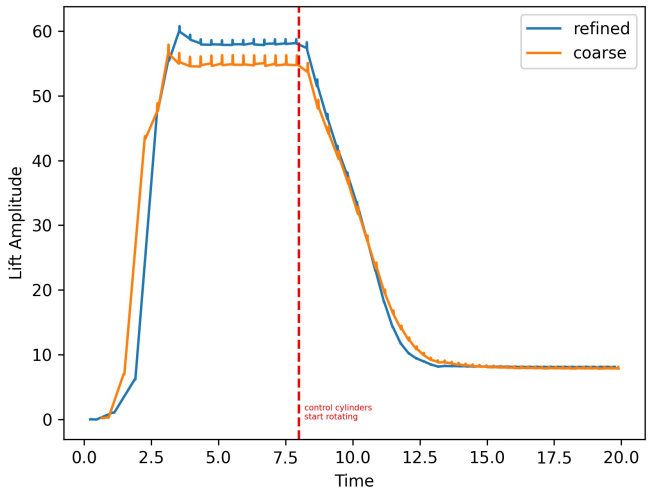

Figure 9: Lift Amplitude behaviour for a coarse and fine grid at Re=1000 and $\xi = 2$

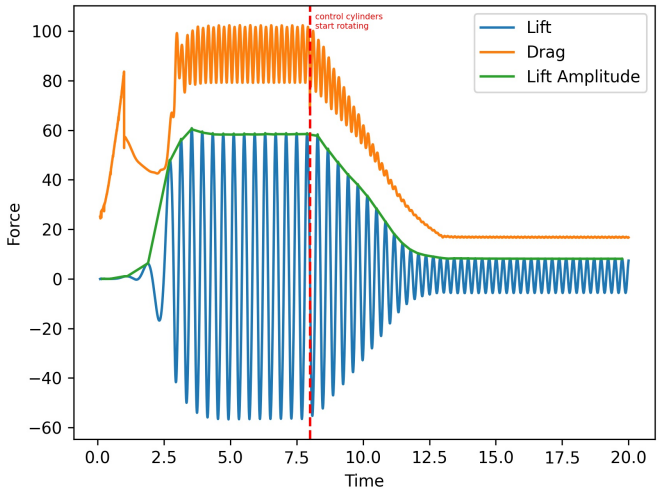

Figure 10: Lift and Drag at Re=1000 and $\xi = 2$. The green line represents the lift amplitude

the flow at a higher angle than without control, the lift oscillations also show a similar trend as the drag. The pressure recovery scales up with the injected momentum into the flow. We saw that at a higher rotating velocity, the steady state with the lower drag and lift amplitude was reached a little earlier. As the control system operates, we notice that the flow starts trending towards potential flow, and the behaviour of the fluid starts behaving like an inviscid fluid.

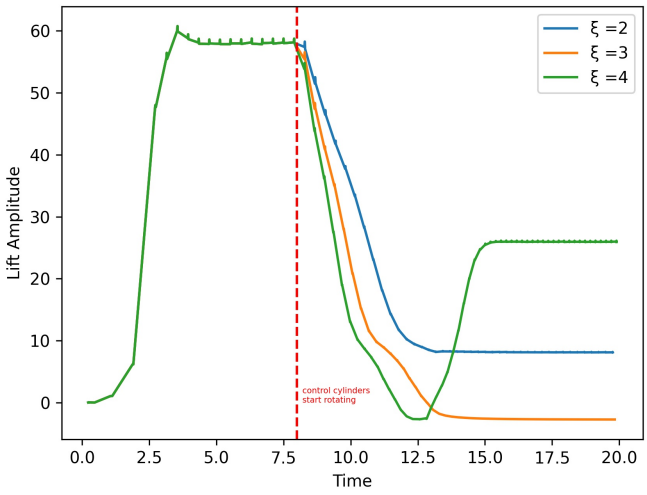

Figure 11: Lift Amplitude vs ξ at Re=1000

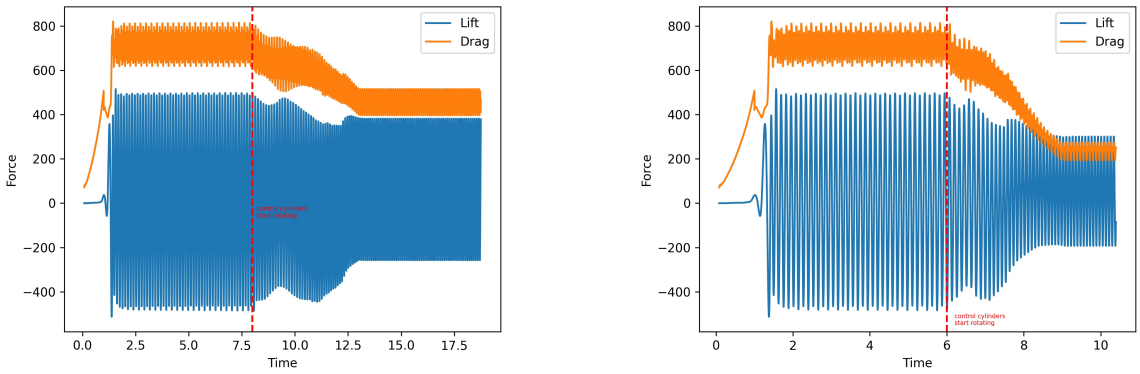

Figure 12: Lift and Drag at Re=3000 and $\xi = 3(left), 5(right)$

References

[1] P.W. Bearman, *Circular cylinder wakes and vortex-induced vibrations*, Journal of Fluids and Structures **27** (2011), no. 5, 648–658, IUTAM Symposium on Bluff Body Wakes and Vortex-Induced Vibrations (BBVIV-6).

[2] I. Korkischko and J.R. Meneghini, *Suppression of vortex-induced vibration using moving surface boundary-layer control*, Journal of Fluids and Structures **34** (2012), 259–270.

[3] S. MITTAL, *Control of flow past bluff bodies using rotating control cylinders*, Journal of Fluids and Structures **15** (2001), no. 2, 291–326.

[4] Sridhar Muddada and B.S.V. Patnaik, *An active flow control strategy for the suppression of vortex structures behind a circular cylinder*, European Journal of Mechanics - B/Fluids **29** (2010), no. 2, 93–104.

[5] James C. Schulmeister, J. M. Dahl, G. D. Weymouth, and M. S. Triantafyllou, *Flow control with rotating cylinders*, Journal of Fluid Mechanics **825** (2017), 743–763.